Title

PTUPB ameliorates high-fat diet-induced non-alcoholic fatty liver disease via inhibiting NLRP3 inflammasome activation in mice

Journal

Biochemical and Biophysical Research Communications, 523(4)

ISSN

0006-291X

Authors

Sun, Chen-Chen

Zhang, Chen-Yu

Duan, Jia-Xi

et al.

Publication Date

2020-03-01

DOI

10.1016/j.bbrc.2019.12.131

Peer reviewed

HHS Public Access

Author manuscript

Biochem Biophys Res Commun. Author manuscript; available in PMC 2021 March 24.

Published in final edited form as:

Biochem Biophys Res Commun. 2020 March 19; 523(4): 1020–1026. doi:10.1016/j.bbrc.2019.12.131.

PTUPB ameliorates high-fat diet-induced non-alcoholic fatty liver disease via inhibiting NLRP3 inflammasome activation in mice

Chen-Chen Sun[1], **Chen-Yu Zhang**[1], **Jia-Xi Duan**[2], **Xin-Xin Guan**[1], **Hui-Hui Yang**[1], **Hui-Ling Jiang**[1], **Bruce D. Hammock**[3], **Sung Hee Hwang**[3], **Yong Zhou**[1], **Cha-Xiang Guan**[1], **Shao-Kun Liu**[2,*], **Jun Zhang**[4,*]

[1]Department of Physiology, Xiangya School of Medicine, Central South University, Changsha, Hunan 410078, China;

[2]Department of Respiratory Medicine, the Second Xiangya Hospital, Central South University, Changsha, Hunan 410011, China;

[3]Department of Entomology and Nematology and UC Davis Comprehensive Cancer Center, University of California, Davis, CA 95616, USA;

[4]Department of Physiology, Hunan University of Medicine, Huaihua, Hunan 418000, China.

Abstract

Non-alcoholic fatty liver disease (NAFLD) affects 25% of the global adult population, and no effective pharmacological treatment has been found. Products of arachidonic acid metabolism have been developed into a novel therapy for metabolic syndrome and diabetes. It has been demonstrated that protective actions of a novel dual cyclooxygenase-2 (COX-2) and soluble epoxide hydrolase (sEH) inhibitor, PTUPB, on the metabolic abnormalities. Here, we investigated the effects of PTUPB on hepatic steatosis in high-fat diet (HFD)-induced obese mice, as well as in hepatocytes *in vitro*. We found that PTUPB treatment reduced body weight, liver weight, liver triglyceride and cholesterol content, and the expression of lipolytic/lipogenic and lipid uptake related genes (*Acc*, *Cd36,* and *Cidec*) in HFD mice. In addition, PTUPB treatment arrested fibrotic progression with a decrease of collagen deposition and expression of Col1a1, Col1a3, and α-SMA. *In vitro*, PTUPB decreased palmitic acid-induced lipid deposition and downregulation of lipolytic/lipogenic genes (*Acc* and *Cd36*) in hepatocytes. Additionally, we found that PTUPB reduced the production of pro-inflammatory cytokines and suppressed the NLRP3 inflammasome activation in HFD mice and hepatocytes. In conclusion, dual inhibition of COX-2/sEH attenuates

[*]**To whom correspondence should be addressed:** Prof. Jun Zhang or Shao-Kun Liu, Hunan University of Medicine, Huaihua, Hunan 418000, China, hhyzzj1314@126.com or shaokunliu228@csu.edu.cn.

Author contributions

SKL and JZ conceived and designed the experiments. CCS, CYZ, JXD, XXG, and HHY performed the experiments. CCS, YFZ, and HLJ analyzed the data. HBD, JZ, and CXG contributed reagents/materials/analysis tools. SHH and BDH designed and synthesized PTUPB. CCS and YZ wrote the paper. CXG, SKL, and JZ critically reviewed the manuscript. All authors had final approval of the submitted versions.

Competing interests

The authors declare no competing financial interests.

Data Availability

The data used to support the findings of this study are available from the corresponding author upon request.

hepatic steatosis by inhibiting NLRP3 inflammasome activation. PTUPB might be a promising potential therapy for liver steatosis associated with obesity.

Keywords

non-alcoholic fatty liver disease; cyclooxygenase-2; soluble epoxide hydrolase; PTUPB; NLRP3 inflammasome

Introduction

Non-alcoholic fatty liver disease (NAFLD), featured by excessive triglyceride accumulation, affects 25% of the global adult population, and the prevalence keeps rising on all continents [1]. NAFLD ranges from simple hepatic lipid accumulation (hepatic steatosis) to non-alcoholic steatohepatitis (NASH) and then leads to hepatocellular carcinoma [2]. NAFLD is strongly associated with arterial hypertension, obesity, insulin resistance, and other obesity-related metabolic disorders [3, 4]. Currently, because the pathogenesis of NAFLD remains unclear, there is no approved pharmacological therapy available for the treatment of this epidemic disease.

Numerous studies show that sterile inflammation is a key trigger for the process of NAFLD [5, 6]. NAFLD is associated with massive release of pro-inflammatory mediators, including tumor necrosis factor-α (TNF-α), interleukin-6 (IL-6) and IL-1β [7]. It has been reported that mild-to-moderate lobular inflammatory cell infiltration was exhibited in the liver tissue of NAFLD rats induced by a high-fat diet (HFD) [8]. The NOD-like receptor family pyrin domain containing 3 (NLRP3) inflammasome drives the sterile inflammation and plays a vital role in the development of NAFLD [9]. Activation of the NLRP3 inflammasome, which can sense a wide range of danger signals, activates caspase-1 and results in the maturation and release of pro-inflammatory cytokines, such as IL-1β and IL-18 [10]. The excessive increase of IL-1β and IL-18 aggravates inflammatory cytokines production and leads to hepatic steatosis and metabolic disorders [11].

The metabolites of arachidonic acid (ARA), which is an abundant lipid mediator in the body, have many different biological functions [12]. Product of ARA metabolism has been developed into a novel therapy for metabolic syndrome and diabetes [13, 14]. Cyclooxygenase-2 (COX-2) is up-regulated in patients or animal models with metabolic syndrome, resulting in accumulation of prostaglandins (PGs) [15, 16]. Accordingly, COX-2 inhibition decreases metabolic syndrome of the kidney in animal models [17]. Epoxyeicosatrienoic acids (EETs), which generate from the ARA by cytochrome P450 (CYP), have anti-inflammatory biological activities [18, 19]. The activity of EETs can be enhanced by blocking their metabolism by soluble epoxide hydrolase (sEH) [20]. Recent research indicates that inhibition of any of the biosynthetic pathway of ARA could switch to the other, leading to fatal side effects [21]. So, we developed a novel dual COX-2/sEH inhibitor, PTUPB [22]. We have reported that the protective actions of this novel dual COX-2/sEH inhibitor on the metabolic abnormalities [23] and pulmonary fibrosis [12]. However, it still unclear whether the dual inhibition of COX-2/sEH has a beneficial action on NAFLD induced by HFD.

Given the anti-inflammatory and anti-metabolic abnormalities effects of dual inhibition of COX-2/sEH and the current limitations in the treatment of NAFLD, we tested the hypothesis that the protective effects of simultaneously inhibiting COX-2 and sEH by PTUPB against HFD-induced NAFLD.

2. Materials and Methods

2.1 Animals experiments

All experiments were approved by the Ethics Committee of Clinical Medicine Research Institute of Central South University (Changsha, China). Adult male C57BL/6 mice (20 ± 2 g) were purchased from Hunan SJA Laboratory Animal Co., Ltd (Hunan, China). All animals were housed in a specific pathogen-free environment and exposed to a 12-h light/dark cycle, with free access to water and a normal diet for one week. Then mice were randomly divided into four groups: the control group (received normal diet), HFD group (received HFD with 60% calories), PTUPB group (5 mg/kg, *s.c.*, daily), and HFD +PTUPB group (received HFD and PTUPB, 5 mg/kg, *s.c.*, daily). Mice were weighed every week. Twelve weeks later, mice were sacrificed, and livers were collected and weighted (Figure 1A).

2.2 Hepatocellular damage assay

Blood samples were isolated. Alanine aminotransferase (ALT) and aspartate aminotransferase (AST) activity, indicators of hepatocellular injury, were measured using the automatic biochemical analyzer (Hitachi automatic biochemical analyzer 7000, Japan).

2.3 Histological analysis

For morphometric studies, liver tissues were fixed in 4% paraformaldehyde solution and embedded in paraffin and cut into 4-μm thick sections. Sections were stained with H&E to observe the tissue morphology or stained with Masson to assess the collagen deposition. Another part of the mouse liver tissue was embedded in the optimal cutting temperature compound (OCT) for Oil Red O staining.

2.4 Triglycerides measurement

Partially frozen mouse liver tissue was taken, weighed, and then physiological saline was added at 1:9. Grinding was carried out under ice bath conditions to prepare a homogenate. After centrifugation at 2500 rpm for 10 min, the supernatant was taken, and the triglyceride (TG) content of the mouse liver tissue was measured according to the TG assay kit (Jiancheng Bioengineering Institute, Nanjing, China).

2.5 Cell culture and treatment

The immortalized mouse normal hepatocyte cell line AML12 was cultured in DMEM/F12 media (Gibco, USA) containing 10% fetal bovine serum, Insulin-Transferrin-Selenium supplement (Gibco, USA), and 40 ng/mL dexamethasone, at 37 °C with 5% CO_2. To investigate the effects of PTUPB on the hepatosteatosis of AML12 cells, we pretreated cells

with PTUPB (1 μM) for 1 h according to a previous study [12], followed by the treatment of palmitic acid (PA, 0.15 mM, and 0.2 mM) for another 12 h.

2.6 Oil red O staining

Take out the frozen slices, re-warm at room temperature for 10 minutes, and then washed with distilled water for 3 minutes to remove the embedding agent. Cell samples were washed twice with PBS and then fixed with 4% paraformaldehyde for 40 minutes. The paraformaldehyde solution was discarded and washed twice with distilled water. After soaking for 2 minutes in 60% isopropanol, slices were stained with Oil Red O working solution (Sigma, USA) for 2 minutes. It was colored with 60% isopropanol, washed with water, then counterstained with hematoxylin and fixed.

2.7 Total RNA extraction and real-time PCR

Total RNA of mouse livers was extracted using Trizol Reagent (Invitrogen) according to the manufacturer's protocol. Then, the RNA was reverse transcribed into cDNA according to the reverse transcription system kit (Takara). Real-time PCR was implemented using SYBR Green (Takara) on the Bio-Rad real-time PCR system (CFX96 Touch™, Bio-Rad, USA). Gene expression levels were calculated by normalizing to β-actin by the $2^{-\Delta\Delta Ct}$ method. Primer sequences used in this study are listed in Table 1.

2.8 Western Blot

As described in our previous study [24]. Frozen mouse liver tissue was taken out and lysed in cold RIPA buffer (Solarbio, Beijing, China) containing a protease inhibitor (Roche, Mannheim, Germany). Protein quantification was performed using a bicinchoninic acid (BCA) protein assay kit (Thermo Fisher Scientific), and the protein (30 mg) in each sample was separated by 12% SDS-PAGE, and then transferred to 0.45-μm polyvinylidene difluoride (PVDF) membranes. The membranes were blocked with 5% fat-free milk and incubated with the primary antibodies overnight at 4°C. Subsequently, membranes were incubated with appropriate secondary HRP-linked antibodies. The proteins were detected with a gel imaging system (Bio-Rad). The antibodies used in present research were as follows: rabbit anti-COX-2 antibody (1:1000, Servicebio, Wuhan, China), rabbit anti-sEH antibody (1:5000, Abcam, USA), rabbit anti-β-tubulin antibody (1:2000, Servicebio), rabbit anti-α-SMA antibody (1:1000, SAB, Maryland, USA), rabbit anti-NLRP3 antibody (1:2000, CST, USA), rabbit anti-pro-caspase-1 antibody (1:1000, Abcam). The expression of protein was normalized to β-tubulin.

2.9 Statistical analysis

Data are expressed as the mean ± SD of three independent experiments. Statistical analysis was processed by GraphPad Prism 7.0 software (San Diego, CA, USA) or SPSS 22.0 (IBM, Chicago, IL). Unpaired *t*-tests were used between the two groups for comparison. The statistical comparisons among the multiple groups were assessed with ANOVA. *Tukey's* test was used as a post hoc test to make pair-wise comparisons. *P*-value < 0.05 was considered statistically significant.

3. Results

3.1 COX-2 and sEH expression are increased in the liver of NAFLD mice

Firstly, we analyzed COX-2 and sEH protein expression in the liver of the HFD-treated mice. We found that both COX-2 and sEH levels in livers of the NAFLD mice were higher than that in the control group (Fig. 1B–C), indicating that dysregulation of ARA metabolism participates in the development of NAFLD. While, treatment with PTUPB significantly reduced COX-2 and sEH protein expression (Fig. 1B–C). These results suggest an important role of liver-expressed COX-2 and sEH dysregulation in the development of NAFLD in mice.

3.2 PTUPB ameliorates HFD-induced NAFLD and fibrosis in mice

Next, we examined whether the dual COX-2 and sEH inhibition had beneficial effects on liver steatosis in an HFD-induced obesity mice model. We found the administration of PTUPB significantly decreased the weight gain compared to the HFD group from the 4^{th} to 12^{th} week (Fig. 2A–D). Oil Red O staining and TG content indicated that PTUPB administration ameliorated hepatosteatosis in HFD mice (Fig. 2E–F). PTUPB lowered the serum ALT and AST levels in the HFD mice, indicating an attenuated liver injury (Fig. 2G–H). Importantly, we detected lipolytic/lipogenic and lipid uptake-related genes, including the key fatty acid synthesis enzyme (*acetyl-CoA carboxylase*, *Acc*), lipid uptake gene (*cluster of differentiation 36*, *Cd36*), and lipid droplet marker (*cell death-inducing DFF45-like effector C*, *Cidec*). We found that PTUPB exhibited an apparent inhibitory effect on these genes (Fig. 2I). In parallel, fibrotic genes (*Col1a1* and *Col3a1*) detection (Fig. 2I), Sirius red staining (Fig. 2J), and α-SMA detection (Fig. 2K) revealed that PTUPB treatment ameliorated the degree of liver fibrosis in the HFD mice. Overall, those data indicate that dual COX-2/sEH inhibition relieves liver steatosis and fibrosis in HFD-induced NAFLD mice.

3.3 PTUPB attenuates NLRP3 inflammasome activation of HFD-induced mice

Inflammation can exacerbate the development of NAFLD [25]. As shown in Fig. 3A–B, the liver of the HFD group exhibited severe inflammatory cell infiltration, while PTUPB treatment remarkably decreased the inflammation score compared with that of the HFD group. Additionally, PTUPB reduced the mRNA expressions of pro-inflammatory factors, including *Tnf-α*, *Mcp-1*, and *IL-6* (Fig. 3C). Accumulating evidence suggests that the NLRP3 inflammasome regulates the maturation and release of IL-1β and IL-18, and contributes to the development of NAFLD [7]. The mRNA expressions of *Nlrp3*, *Asc*, *pro-caspase-1*, *pro-IL-1β*, and *pro-IL-18* in liver tissues of HFD mice were decreased after treatment with PTUPB (Fig. 3D). As expected, PTUPB significantly reduced the NLRP3, pro-caspase-1, and caspase-1 p17 protein expression (Fig. 3E). These results indicate that PTUPB exerts an anti-inflammatory effect against HFD-induced inflammation in mice, maybe via inhibiting the NLRP3 inflammasome activation.

3.4 PTUPB alleviates hepatosteatosis in a mouse hepatic cell line in vitro

To affirm the observation *in vivo*, we treated hepatocyte AML12 cells with PA for 12 h. We found that PTUPB significantly reduced *Cox-2* mRNA expression induced by PA treatment

(Fig. 4A). PTUPB also remarkably decreased PA-induced lipid deposition in AML12 cells, as revealed by Oil red O staining (Fig. 4B). PA-induced upregulation of lipolytic/lipogenic and lipid uptake-related genes (*Acc* and *Cd36*) and inflammation-related genes (*Tnf-α* and *Il-6*) were suppressed by PTUPB administration in AML12 cells (Fig. 4C–D). Additionally, PTUPB reduced the mRNA levels of NLRP3 inflammasome-associated genes (*Nlrp3*, *Asc*, *pro-caspase-1*, and *pro-IL-18*) induced by PA (Fig. 4E). These data strongly suggest an inhibitory role of PTUPB on hepatosteatosis and inflammation in mouse hepatocytes *in vitro*.

Discussion

In the present study, we explored new potential therapeutic effects of dual COX-2/sEH inhibition by PTUPB, which can ameliorate hepatic steatosis in obese mice. The anti-steatosis effects of PTUPB may result from the suppression of NLRP3 inflammasome activation. Our data indicate that dual inhibition of COX-2/sEH might be an effective treatment for obesity-associated hepatosteatosis associated with obesity.

PTUPB simultaneously acts on COX-2 and sEH pathways of ARA metabolism, which has many pharmacological activities, such as anti-cancer and anti-fibrosis [12, 26]. It is reported that PTUPB inhibits allergen-induced airway inflammation by inhibiting eosinophilic infiltration and increasing levels of anti-inflammatory EETs in the lung tissue [27]. PTUPB also can attenuate kidney injury *via* reducing renal inflammation and oxidative stress in type 2 diabetic Zucker diabetic fatty rats [23]. NAFLD is commonly associated with metabolic comorbidities with no approved pharmacologic agents currently [2, 28]. In this study, we reported that COX-2 and sEH levels were increased in the livers of NAFLD mice, as well as the expression of the lipolytic/lipogenic and lipid uptake related genes. ACC active produces malonyl-CoA, blocks the production of new fatty acids, and inhibits the transfer of the fatty acyl group from acyl CoA to carnitine with carnitine acyltransferase [29]. CD36 contributes to intracellular lipid accumulation [30]. CIDEC participates in the differentiation of adipocyte adipogenesis [31]. Here, we found that PTUPB significantly reduced *Acc*, *Cd36*, and *Cidec* expression. Moreover, PTUPB treatment decreased the body weight, liver weight, and serum levels of TG of mice in the HFD group. In addition, the generation of liver fibrosis in NAFLD, which is a key feature of progressive disease [32]. Based on those findings, we proposed a new therapeutic potential for NAFLD.

Inflammation is considered vital pathogenesis of the majority of acute and chronic liver diseases, such as NAFLD and alcoholic fatty liver disease [25, 33]. It has been pointed out that low-grade chronic inflammation of NAFLD is a link to hepatic lipid accumulation [34]. The inflammatory gene expression in the liver is increased in NAFLD mice, such as IL-1β, IL-18, IL-6, and TNF-α [7, 35]. Herein, we found that PTUPB suppressed the expression of pro-inflammatory cytokines in livers of NAFLD mice, including *Tnf-α*, *Mcp-1*, and, *IL-6*. Accumulating evidence demonstrate that NLRP3 inflammasome is an indispensable contributor to the development of NAFLD [36, 37]. NLRP3 inflammasome, which is activated by metabolic danger signals, form the complex of the NLRP3 inflammasome by recruiting ASC together with pro-caspase-1, subsequently leading to cleaves pro-IL-1β and pro-IL-18 into active forms [10]. In this study, we found that PTUPB treatment effectively

suppressed the overexpression of NLRP3 and inhibited the activation of the NLRP3 inflammasome in the liver of HFD-fed mice. The *in vitro* study further confirmed that PTUPB could inhibit the activation of NLRP3 inflammasome in PA-treated hepatocyte. In other animal model, PTUPB also shows anti-inflammatory property. For example, PTUPB protects against allergen-induced bronchoconstriction and airway inflammation in asthma [27]. To the best knowledge of us, this is the first study indicating PTUPB could inhibit the activation of the NLRP3 inflammasome.

In conclusion, this study suggests that dual inhibition of COX-2/sEH attenuates hepatic steatosis by inhibiting the NLRP3 inflammasome activation *in vitro* and *in vivo*. And dual inhibition of COX-2/sEH might be a promising potential therapy for liver steatosis associated with obesity, though its potential in human disease remains unproven.

Acknowledgments

This study was supported by the National Natural Science Foundation of China (81670014), the Hunan Provincial Natural Science Foundation of China (2019JJ40453, 2016JJ6107), and the Research Foundation of Education Bureau of Hunan Province, China (16A153).

References

[1]. Liu T, Luo X, Li ZH, Wu JC, Luo SZ, Xu MY, Zinc-alpha2-glycoprotein 1 attenuates non-alcoholic fatty liver disease by negatively regulating tumour necrosis factor-alpha, World journal of gastroenterology, 25 (2019) 5451–5468. [PubMed: 31576092]

[2]. Starley BQ, Calcagno CJ, Harrison SA, Nonalcoholic fatty liver disease and hepatocellular carcinoma: a weighty connection, Hepatology (Baltimore, Md.), 51 (2010) 1820–1832.

[3]. Chalasani N, Younossi Z, Lavine JE, Charlton M, Cusi K, Rinella M, Harrison SA, Brunt EM, Sanyal AJ, The diagnosis and management of nonalcoholic fatty liver disease: Practice guidance from the American Association for the Study of Liver Diseases, Hepatology (Baltimore, Md.), 67 (2018) 328–357.

[4]. Birkenfeld AL, Shulman GI, Nonalcoholic fatty liver disease, hepatic insulin resistance, and type 2 diabetes, Hepatology (Baltimore, Md.), 59 (2014) 713–723.

[5]. Kubes P, Mehal WZ, Sterile inflammation in the liver, Gastroenterology, 143 (2012) 1158–1172. [PubMed: 22982943]

[6]. Lu Y, Jiang Z, Dai H, Miao R, Shu J, Gu H, Liu X, Huang Z, Yang G, Chen AF, Yuan H, Li Y, Cai J, Hepatic leukocyte immunoglobulin-like receptor B4 (LILRB4) attenuates nonalcoholic fatty liver disease via SHP1-TRAF6 pathway, Hepatology (Baltimore, Md.), 67 (2018) 1303–1319.

[7]. Wang F, Liu Y, Yuan J, Yang W, Mo Z, Compound C protects mice from HFD-induced obesity and nonalcoholic fatty liver disease, International journal of endocrinology, 2019 (2019) 3206587. [PubMed: 31485221]

[8]. El-Din SH, Sabra AN, Hammam OA, Ebeid FA, El-Lakkany NM, Pharmacological and antioxidant actions of garlic and.or onion in non-alcoholic fatty liver disease (NAFLD) in rats, Journal of the Egyptian Society of Parasitology, 44 (2014) 295–308. [PubMed: 25597144]

[9]. Neumann K, Schiller B, Tiegs G, NLRP3 inflammasome and IL-33: Novel players in sterile liver inflammation, International journal of molecular sciences, 19 (2018) E2732. [PubMed: 30213101]

[10]. Strowig T, Henao-Mejia J, Elinav E, Flavell R, Inflammasomes in health and disease, Nature, 481 (2012) 278–286. [PubMed: 22258606]

[11]. Schroder K, Tschopp J, The inflammasomes, Cell, 140 (2010) 821–832. [PubMed: 20303873]

[12]. Zhang CY, Duan JX, Yang HH, Sun CC, Zhong WJ, Tao JH, Guan XX, Jiang HL, Hammock BD, Hwang SH, Zhou Y, Guan CX, COX-2/sEH dual inhibitor PTUPB alleviates bleomycin-induced pulmonary fibrosis in mice via inhibiting senescence, The FEBS journal, (2019).

[13]. Kim GH, Renal effects of prostaglandins and cyclooxygenase-2 inhibitors, Electrolyte & blood pressure : E & BP, 6 (2008) 35–41. [PubMed: 24459520]

[14]. He J, Wang C, Zhu Y, Ai D, Soluble epoxide hydrolase: A potential target for metabolic diseases, Journal of diabetes, 8 (2016) 305–313. [PubMed: 26621325]

[15]. Vessieres E, Belin de Chantemele EJ, Toutain B, Guihot AL, Jardel A, Loufrani L, Henrion D, Cyclooxygenase-2 inhibition restored endothelium-mediated relaxation in old obese zucker rat mesenteric arteries, Frontiers in physiology, 1 (2010) 145. [PubMed: 21423385]

[16]. Robertson RP, The COX-2/PGE2/EP3/Gi/o/cAMP/GSIS pathway in the Islet: The beat goes on, Diabetes, 66 (2017) 1464–1466. [PubMed: 28533298]

[17]. Imig JD, Zhao X, Dey A, Shaw M, CYP450, COX-2 and obesity related renal damage, Toxicology mechanisms and methods, 15 (2005) 125–136. [PubMed: 20021073]

[18]. Zhou Y, Liu T, Duan JX, Li P, Sun GY, Liu YP, Zhang J, Dong L, Lee KSS, Hammock BD, Jiang JX, Guan CX, Soluble epoxide hydrolase inhibitor attenuates lipopolysaccharide-induced acute lung injury and improves survival in mice, Shock, 47 (2017) 638–645. [PubMed: 27753791]

[19]. Zarriello S, Tuazon JP, Corey S, Schimmel S, Rajani M, Gorsky A, Incontri D, Hammock BD, Borlongan CV, Humble beginnings with big goals: Small molecule soluble epoxide hydrolase inhibitors for treating CNS disorders, Progress in neurobiology, 172 (2019) 23–39. [PubMed: 30447256]

[20]. Sun H, Lee P, Yan C, Gao N, Wang J, Fan X, Yu FS, Inhibition of soluble epoxide hydrolase 2 ameliorates diabetic keratopathy and impaired wound healing in mouse corneas, Diabetes, 67 (2018) 1162–1172. [PubMed: 29615440]

[21]. P JJ, Manju SL, Ethiraj KR, Elias G, Safer anti-inflammatory therapy through dual COX-2/5-LOX inhibitors: A structure-based approach, Eur J Pharm Sci, 121 (2018) 356–381. [PubMed: 29883727]

[22]. Hwang SH, Wagner KM, Morisseau C, Liu JY, Dong H, Wecksler AT, Hammock BD, Synthesis and structure-activity relationship studies of urea-containing pyrazoles as dual inhibitors of cyclooxygenase-2 and soluble epoxide hydrolase, J Med Chem, 54 (2011) 3037–3050. [PubMed: 21434686]

[23]. Hye Khan MA, Hwang SH, Sharma A, Corbett JA, Hammock BD, Imig JD, A dual COX-2/sEH inhibitor improves the metabolic profile and reduces kidney injury in Zucker diabetic fatty rat, Prostaglandins & other lipid mediators, 125 (2016) 40–47. [PubMed: 27432695]

[24]. Zhong WJ, Yang HH, Guan XX, Xiong JB, Sun CC, Zhang CY, Luo XQ, Zhang YF, Zhang J, Duan JX, Zhou Y, Guan CX, Inhibition of glycolysis alleviates lipopolysaccharide-induced acute lung injury in a mouse model, Journal of cellular physiology, 234 (2019) 4641–4654. [PubMed: 30256406]

[25]. Cortez-Pinto H, de Moura MC, Day CP, Non-alcoholic steatohepatitis: from cell biology to clinical practice, J Hepatol, 44 (2006) 197–208. [PubMed: 16274837]

[26]. Gartung A, Yang J, Sukhatme VP, Bielenberg DR, Fernandes D, Chang J, Schmidt BA, Hwang SH, Zurakowski D, Huang S, Kieran MW, Hammock BD, Panigrahy D, Suppression of chemotherapy-induced cytokine/lipid mediator surge and ovarian cancer by a dual COX-2/sEH inhibitor, Proceedings of the National Academy of Sciences of the United States of America, 116 (2019) 1698–1703. [PubMed: 30647111]

[27]. Daham K, James A, Balgoma D, Kupczyk M, Billing B, Lindeberg A, Henriksson E, FitzGerald GA, Wheelock CE, Dahlen SE, Dahlen B, Effects of selective COX-2 inhibition on allergen-induced bronchoconstriction and airway inflammation in asthma, J Allergy Clin Immunol, 134 (2014) 306–313. [PubMed: 24461582]

[28]. Farrell GC, Larter CZ, Nonalcoholic fatty liver disease: from steatosis to cirrhosis, Hepatology (Baltimore, Md.), 43 (2006) S99–S112.

[29]. Xiao XH, Wang YD, Qi XY, Wang YY, Li JY, Li H, Zhang PY, Liao HL, Li MH, Liao ZZ, Yang J, Xu CX, Wen GB, Liu JH, Zinc alpha2 glycoprotein protects against obesity-induced hepatic steatosis, International journal of obesity (2005), 42 (2018) 1418–1430. [PubMed: 30006580]

[30]. Sheng D, Zhao S, Gao L, Zheng H, Liu W, Hou J, Jin Y, Ye F, Zhao Q, Li R, Zhao N, Zhang L, Han Z, Wei L, BabaoDan attenuates high-fat diet-induced non-alcoholic fatty liver disease via activation of AMPK signaling, Cell & bioscience, 9 (2019) 77. [PubMed: 31548878]

[31]. Lebeaupin C, Vallee D, Rousseau D, Patouraux S, Bonnafous S, Adam G, Luciano F, Luci C, Anty R, Iannelli A, Marchetti S, Kroemer G, Lacas-Gervais S, Tran A, Gual P, Bailly-Maitre B, Bax inhibitor-1 protects from nonalcoholic steatohepatitis by limiting inositol-requiring enzyme 1 alpha signaling in mice, Hepatology (Baltimore, Md.), 68 (2018) 515–532.

[32]. Dowman JK, Tomlinson JW, Newsome PN, Pathogenesis of non-alcoholic fatty liver disease, QJM : monthly journal of the Association of Physicians, 103 (2010) 71–83. [PubMed: 19914930]

[33]. Racanelli V, Rehermann B, The liver as an immunological organ, Gastroenterology, 43 (2004) S54–62.

[34]. Xu B, Jiang MZ, Chu Y, Wang WJ, Chen D, Li XW, Zhang Z, Zhang D, Fan DM, Nie YZ, Shao F, Wu KC, Liang J, Gasdermin D plays a key role as a pyroptosis executor of non-alcoholic steatohepatitis in humans and mice, Journal of Hepatology, 68 (2018) 773–782. [PubMed: 29273476]

[35]. Feldmann M, Maini RN, Lasker Clinical Medical Research Award. TNF defined as a therapeutic target for rheumatoid arthritis and other autoimmune diseases, Nature medicine, 9 (2003) 1245–1250.

[36]. Wree A, Eguchi A, McGeough MD, Pena CA, Johnson CD, Canbay A, Hoffman HM, Feldstein AE, NLRP3 inflammasome activation results in hepatocyte pyroptosis, liver inflammation, and fibrosis in mice, Hepatology (Baltimore, Md.), 59 (2014) 898–910.

[37]. Henao-Mejia J, Elinav E, Jin C, Hao L, Mehal WZ, Strowig T, Thaiss CA, Kau AL, Eisenbarth SC, Jurczak MJ, Camporez JP, Shulman GI, Gordon JI, Hoffman HM, Flavell RA, Inflammasome-mediated dysbiosis regulates progression of NAFLD and obesity, Nature, 482 (2012) 179–185. [PubMed: 22297845]

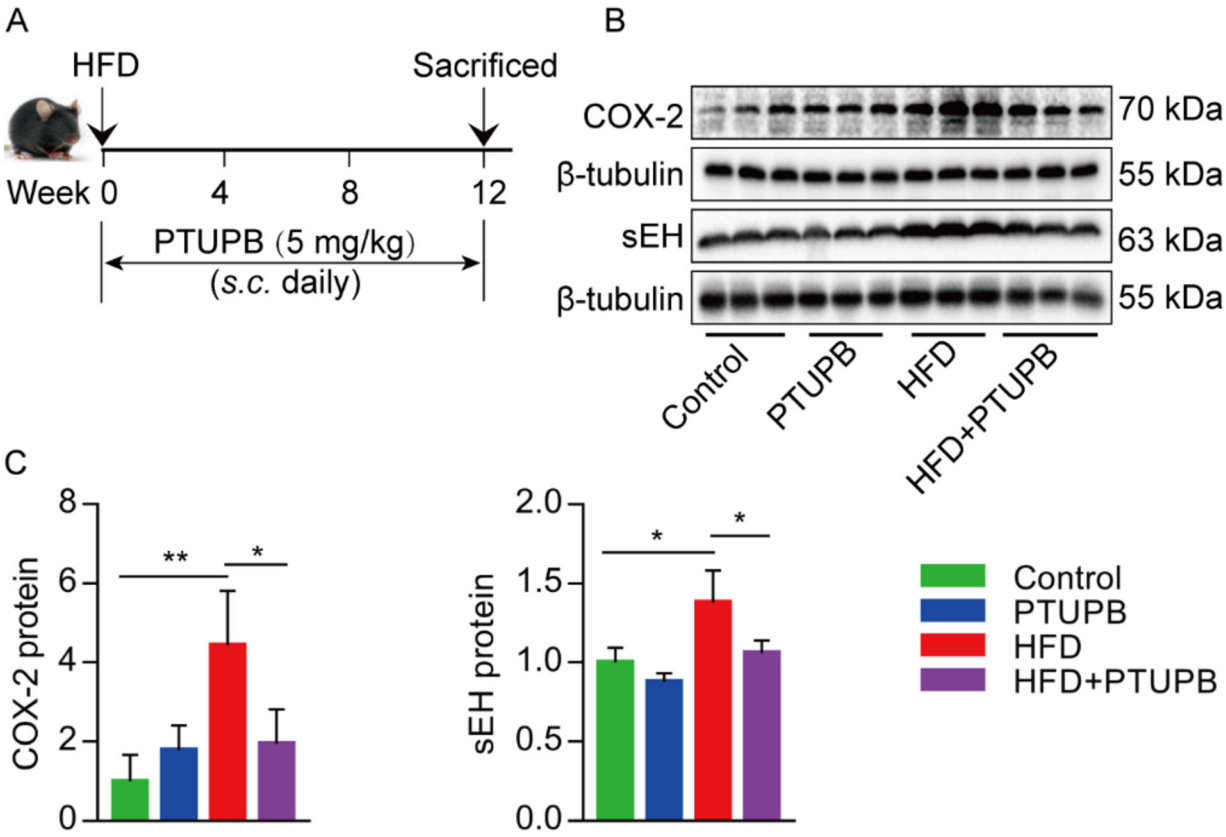

Figure 1. COX-2 and sEH expression are increased in the liver of NAFLD mice.

(A) C57BL/6 mice were fed with HDF with or without subcutaneous injection of PTUPB (5 mg/kg) for 12 weeks. (B-C) COX-2 and sEH protein expressions in liver tissue were detected using western blot. Data are shown as the mean ± SD ($n = 8$). * $P < 0.05$ and ** $P < 0.01$.

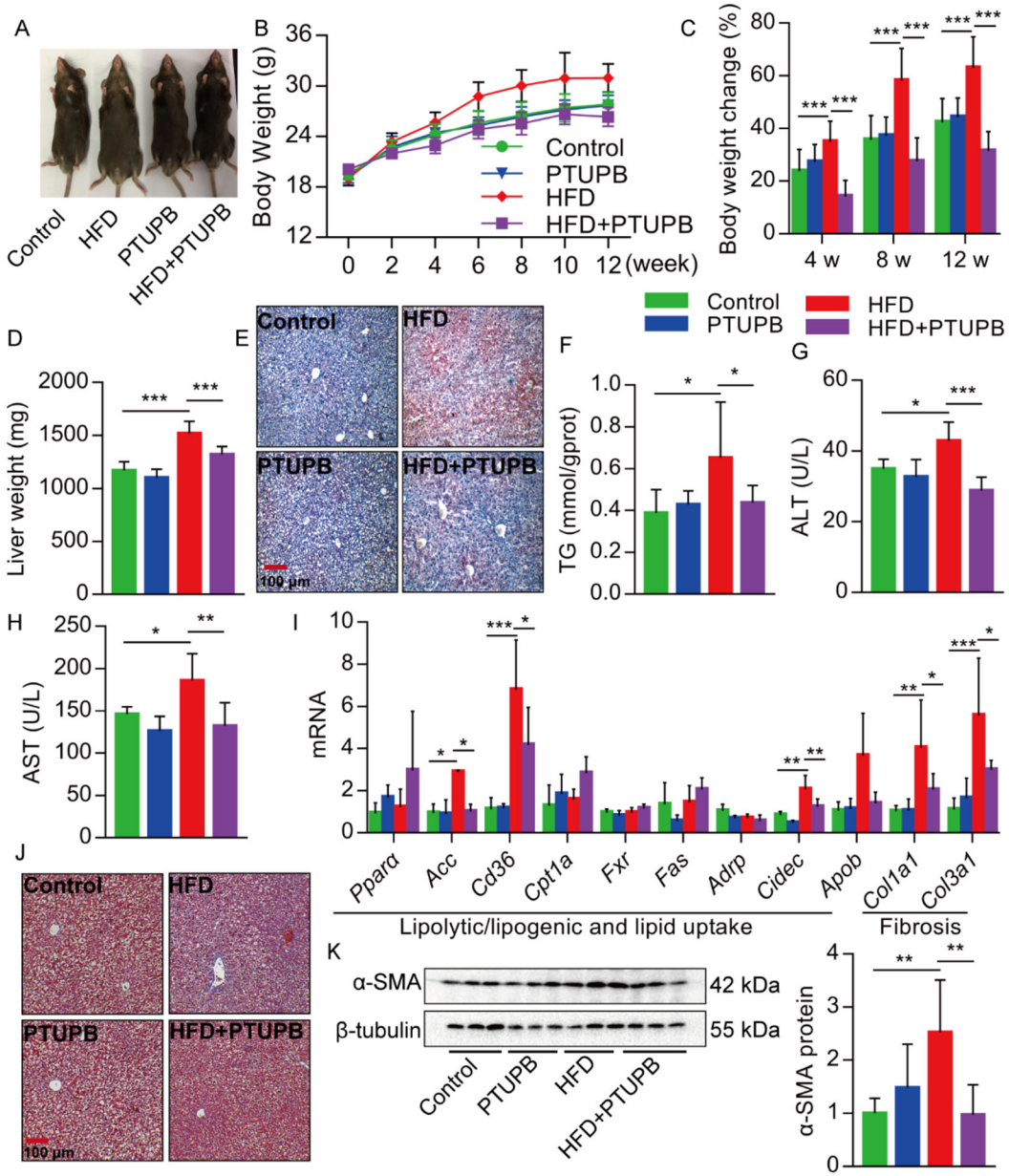

Figure 2. PTUPB ameliorates HFD-induced NAFLD and liver fibrosis in mice.

(A) Representative images of mice fed with HFD with or without PTUPB. (B-D) The change of body weight and liver weight of mice after HDF treatment for 12 weeks with or without PTUPB. (E) Representative photomicrographs of liver sections stained with Oil Red O. Scale bars = 100 μm. (F-H) Content of TG in liver tissue and activity of ALT and AST in the serum of mice. (I) The expression of lipolytic/lipogenic and lipid uptake-related genes (*Pparα*, *Acc*, *Cd36*, *Cpt1a*, *Fxr*, *Fas*, *Adrp*, *Cidec*, and *Apob*) and fibrotic genes (*Col1a1* and *Col3a1*) in liver tissue were detected using real-time PCR. (J) Representative photomicrographs of liver sections stained with Masson's trichrome. Scale bars = 100 μm. (K) α-SMA protein expression in liver tissue was detected using western blot. Data are shown as the mean ± SD ($n = 8$). * $P < 0.05$, ** $P < 0.01$, and *** $P < 0.001$.

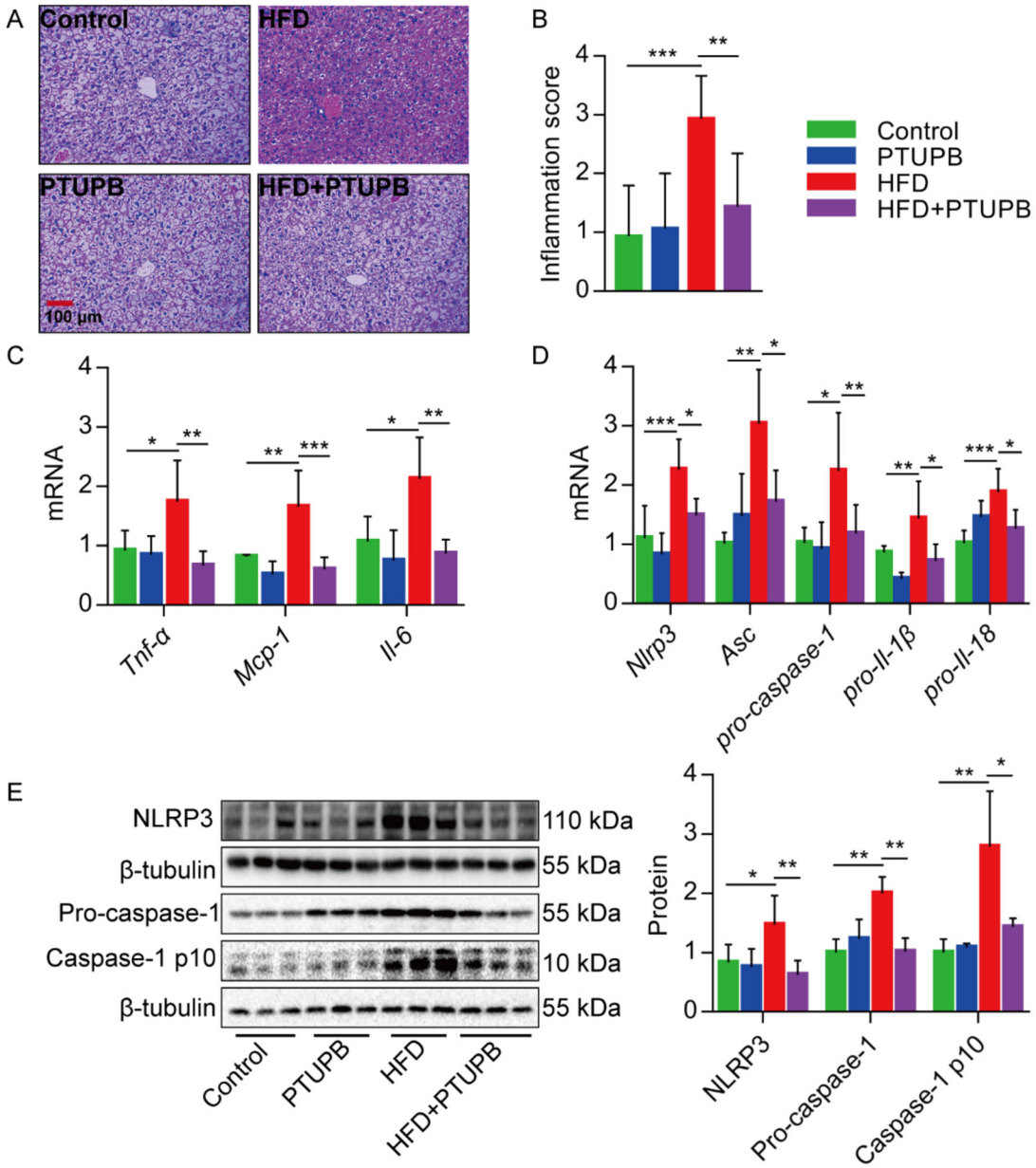

Figure 3. PTUPB attenuates liver inflammation and inhibits the NLRP3 inflammasome activation of HFD-induced mice.

(A) Representative photomicrographs of liver sections stained with H&E. Scale bars = 100 μm. (B) Inflammation score (based on H&E staining) expressed on a numerical scale. (C) *Tnf-α*, *Mcp-1*, and *Il-6* mRNA expression in liver tissue were detected using real-time PCR. (D) *Nlrp3*, *Asc*, *pro-caspase-1*, *pro-IL-1β*, and *pro-IL-18* mRNA expression in liver tissue were detected using real-time PCR. (E) NLRP3, pro-caspase-1, and caspase-1 p10 protein expression in liver tissue were detected using western blot ($n = 8$). Data are shown as the mean ± SD. * $P < 0.05$, ** $P < 0.01$, and *** $P < 0.001$.

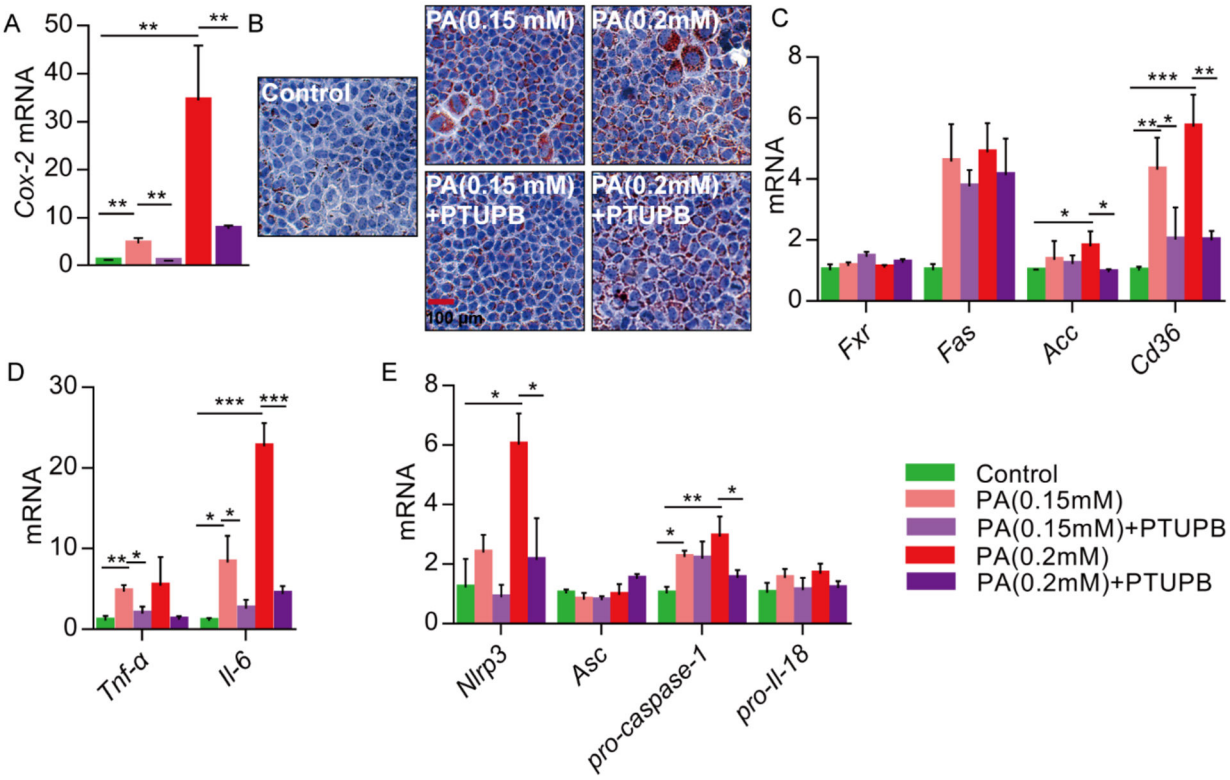

Figure 4. PTUPB alleviates hepatosteatosis in a mouse hepatic cell line *in vitro*.

PTUPB (1 μM) was added to PA (0.15 mM or 0.2 mM)-challenged AML12 cells. Twelve hours later, *Cox-2* mRNA (A) in AML12 cells were determined using real-time PCR. (B) Representative photomicrographs of AML12 cells stained with Oil Red O. Scale bars = 100 μm. (C) *Fxr*, *Fas*, *Acc*, and *Cd36* mRNA in AML12 cells were determined using real-time PCR. (D) *Tnf-α* and *Il-6* mRNA expression in AML12 cells were detected. (E) *Nlrp3*, *Asc*, *pro-caspase-1,* and *pro-Il-18* mRNA expression in AML12 cells were detected. Data are expressed as the mean ± SD ($n = 5$). * $P < 0.05$, ** $P < 0.01$, and *** $P < 0.001$.

Table 1.

Primer sequences used in this study

Gene	Forward primer (5′–3′)	Reverse primer (5′–3′)
Pparα	gctcactgttttcgtggttgta	gactctgttttctgggctcttc
Acc	tctcctccaacctcaaccac	aagcagcccatcacttcatc
Cd36	gaaccactgctttcaaaaactgg	tgctgttctttgccacgtca
Cptia	cgctactccctgaaagtg	cttgaccatacccatccag
Fxr	ggcagaatctggatttggaatcg	gcccaggttggaatagtaagacg
Fas	tgcgtggcctttgaaatgtgct	acacgctcctctaggcccttca
Adrp	gtggtctgagcaggcttcat	agggaaggaaaaacctcacctc
Cidec	gggggaggtccaacacaatc	gggtacaggaggctgagaga
Apob	aagaccatcctgagccagac	ggtcttggttcttatgccagc
Col1a1	gagcggagagtactggatcg	gcttcttttccttggggttc
Col3a1	gcacagcagtccaacgtaga	tctccaaatgggatctctgg
Tnf-α	*agcccccagtctgtatcctt*	*ctccctttgcagaactcagg*
Mcp-1	*gtccctgtcatgcttctgg*	*gcgttaactgcatctggct*
Il-6	cggccttccctacttcacaa	tgtgactccagcttatctcttgg
Nlrp3	*tacggccgtctacgtcttct*	*cgcagatcacactcctcaaa*
Asc	gacagtaccaggcagttcgt	agtccttgcaggtcaggttc
pro-Il-1β	caggcaggcagtatcactca	agctcatatgggtccgacag
pro-Il-18	acgtgttccaggacacaaca	caaaccctccccacctaact
pro-caspase-1	cacagctctggagatggtga	ctttcaagcttgggcacttc
Cox2	*catccccttcctgcgaagtt*	*catgggagttgggcagtcat*
β-actin	*ttccagccttccttcttg*	*ggagccagagcagtaatc*